Heliyon 9 (2023) e18290

Contents lists available at ScienceDirect

Heliyon

journal homepage: www.cell.com/heliyon

Circular RNA circSLC7A11 contributes to progression and stemness of laryngeal squamous cell carcinoma via sponging miR-877-5p from LASP1

Wenjie Yu, Xiaoling He, Chunming Zhang, Fuhui Huang *

Department of Otolaryngology Head and Neck Surgery, First Hospital of Shanxi Medical University, China

ARTICLE INFO

Keywords:
CircSLC7A11
LSCC
miR-877-5p
LASP1

ABSTRACT

Background: Laryngeal squamous cell carcinoma (LSCC) belongs to tumors of head and neck. Circular RNA circSLC7A11 functions as oncogenes in various tumors. However, the role of circSLC7A11 in LSCC remains largely unknown. Here, we aimed to clarify the circSLC7A11 function in LSCC.

Methods: Relevance between circSLC7A11 expressions and LSCC clinicopathological was checked using chi-square. Relevance between circSLC7A11 expressions and LSCC patients' survival time was validated using Kaplan-Meier analysis. CircSLC7A11 expressions in LSCC tissues and cells were determined using quantitative real-time PCR. CircSLC7A11 functions in LSCC were examined by Cell Counting Kit-8, EdU analysis, Western blot, flow cytometry, sphere formation assay, and Transwell analysis. Meanwhile, circSLC7A11 mechanism in LSCC was determined using dual-luciferase reporter analysis, RNA pull-down, RNA Immunoprecipitation.

Results: CircSLC7A11 was highly expressed in LSCC, and high circSLC7A11 expressions were interrelated to the TNM stage. Also, LSCC patients with high circSLC7A11 owned shorter overall survival. Functional studies revealed that circSLC7A11 knockdown reduced LSCC cell proliferation, migration, invasion, stemness characteristics, and enhanced cell apoptosis. Mechanistic study data corroborated that circSLC7A11 targeted miR-877-5p, miR-877-5p targeted LASP1. LASP1 was negatively interrelated to miR-877-5p and was positively interrelated to circSLC7A11 in LSCC tissues. Also, circSLC7A11 knockdown reduced the LASP1 levels, and miR-877-5p inhibitor co-transfection reversed this reduction. Rescue assays further demonstrated that circSLC7A11 accelerated LSCC through miR-877-5p/LASP1.

Conclusion: CircSLC7A11 exerted oncogenic functions in LSCC by miR-877-5p/LASP1, hinting that circSLC7A11 was a novel biomarker for LSCC.

1. Introduction

Laryngeal squamous cell carcinoma (LSCC) is a laryngeal cancer subtype and head and neck tumor that brings pressure on the healthcare system worldwide [1]. Risk factors for LSCC contain tobacco smoking and alcohol consumption [2]. LSCC onset is insidious, and patients (nearly 60%) are usually already in advanced stage (clinical stages III and IV) once they are diagnosed [3,4]. At present, some progress has been made in LSCC intervention containing radiotherapy, surgery, and chemotherapy, but LSCC patients' prognosis

* Corresponding author. No. 85, Jiefang South Road, Yingze District, Taiyuan City 030001, Shanxi Province, China.
E-mail address: huangfuhuisx@126.com (F. Huang).

https://doi.org/10.1016/j.heliyon.2023.e18290
Received 18 January 2023; Received in revised form 10 July 2023; Accepted 13 July 2023
Available online 14 July 2023

is still unsatisfactory [5]. Therefore, revealing LSCC evolution underlying mechanisms is momentous to provide promising targets for LSCC.

Circular RNAs (circRNAs) are an abundant class of non-coding RNAs discovered in recent years [6]. Due to the special structure of circRNAs, circRNAs are more stable and guarantee high conservation of circRNAs [7,8]. CircRNAs are usually generated by noncanonical post-splicing events [9], and they are initially thought to be aberrant by-products and have only been demonstrated to have cellular functions in recent years [10]. Accumulated evidence suggests that circRNAs have multiple functions, such as miRNAs sponges, and mediating protein translation [11]. Crucially, circular RNAs have been proven to be markers of tumorigenesis including LSCC. For instance, Fan et al. illustrated that LSCC patients with high circ_0120175 expressions are interrelated to tumor stage, survival time, and circ_0120175 loss reduces LSCC growth [12]. Chen et al. verified that circ_0001883 is abnormally overexpressed in LSCC, and circ_0001883 loss reduces LSCC growth via PI3K/AKT [13]. Additionally, circSLC7A11 (circBase ID: hsa_circ_0070975) originates exons 8, and 9 of *SLC7A11* [14]. CircSLC7A11 exerts roles in several tumors, such as hepatocellular carcinoma [14], and bone cancer [15]. So far, circSLC7A11 function in LSCC was undefined. In the research, we preliminarily confirmed abnormally high expressions of circSLC7A11 in LSCC, hinting that circSLC7A11 might participate in mediating LSCC evolution. This research next focused on circSLC7A11 mechanism in influencing LSCC.

In this research, we preliminarily confirmed a novel up-regulated circSLC7A11 in LSCC tissues. Meanwhile, we corroborated that circSLC7A11 expressions were increased in LSCC (TNM stage III) in comparison with TNM stage I + II, and LSCC patients with high circSLC7A11 owned short overall survival. These studies suggested that circSLC7A11 might function as an oncogene in LSCC. On this basis, we continue to illustrate circSLC7A11 potential mechanism in accelerating LSCC process, aiming to effective therapeutic markers for LSCC clinical therapy.

2. Materials and methods

2.1. Bioinformatics analysis

Relevance between circSLC7A11 and miR-877-5p, LASP1 and miR-877-5p was forecasted via StarBase (http://starbase.sysu.edu.cn/) given previously reported methods [16].

2.2. Human tissues

Patients diagnosed with LSCC (n = 68) were from First Hospital of Shanxi Medical University. All patients were aware of experimental details and clinical tissue application was under LSCC patient's consent. Experiments were agreed upon with the Ethics Committee of First Hospital of Shanxi Medical University.

2.3. Cell culture

LSCC cells TU686, AMC–HN–8 (with high invasion), and human nasopharyngeal epithelial cells (NP69) were provided by ATCC (Maryland, USA). Detail information for TU686, AMC–HN–8, and NP69 cells was provided in Cellosaurus online database (TU686: https://www.cellosaurus.org/CVCL_4916, AMC–HN–8: https://www.cellosaurus.org/CVCL_5966 and NP69: https://www.cellosaurus.org/CVCL_F755).

TU686 and AMC–HN–8 cells were kept in DMEM with 10% FBS (Procell, Wuhan, China), and 1% penicillin/streptomycin (Procell). NP69 cells were kept in RPMI-1640 with 10% FBS and 1% penicillin/streptomycin. All cells were grown at 37 °C, 5% CO_2.

2.4. Cell transfection

Sh-circSLC7A11#1, sh-circSLC7A11#2, sh-circSLC7A11#3, si-LASP1#1, si-LASP1#2, si-LASP1#3 or pcDNA-circSLC7A11 were from Genechem (Shanghai, China). MiR-877-5p mimic or inhibitor was supplied by RiboBio.

LSCC cells (5×10^5) were grown in 6-well plates for 1 d. Synthesized sh-circSLC7A11#1, sh-circSLC7A11#2, sh-circSLC7A11#3,

Table 1
Primer sequences.

Gene name	Primer sequence (5′-3′)
CircSLC7A11	Forward: TTGTTTTGACCTTTTCTGAGC
	Reverse: AACACACCACCGTTCATGG
MiR-877-5p	Forward: GCCGTAGAGGAGATGGC
	Reverse: CAGTGCGTGTCGTGGA
LASP1	Forward: GTGTATCCCACGGAGAAGGT
	Reverse: TGCCACTACGCTGAAACCT
GAPDH	Forward: GGAGCGAGATCCCTCCAAAAT
	Reverse: GGCTGTTGTCATACTTCTCATGG
U6	Forward: CTCGCTTCGGCAGCACA
	Reverse: AACGCTTCACGAATTTGCGT

si-LASP1#1, si-LASP1#2, si-LASP1#3, pcDNA-circSLC7A11, miR-877-5p mimic, or inhibitor was transfected to LSCC cells using Lipofectamine 3000 (ThermoFisher Scientific, Massachusetts, USA) [17].

2.5. Quantitative real-time PCR

Total RNA was extracted with TRIzol (ThermoFisher Scientific). For circSLC7A11 and LASP1 analysis, complementary DNA was synthesized by SuperScriptIII reverse transcriptase (ThermoFisher Scientific). For miR-877-5p analysis, complementary DNA was obtained using Mir-X miRNA First-Strand Synthesis Kits (TaKaRa, Dalian, China). Then, real-time PCR was conducted on LightCycler 96 Instrument with SYBR Green I (Solarbio, Beijing, China). PCR reaction was listed as follows: 95 °C 2 min; 35 cycles, 95 °C 25 s; 60 °C 25 s, and 72 °C 1 min. Relative level was determined with $2^{-\Delta\Delta Ct}$. Primer sequences were exhibited in Table 1.

2.6. Cell Counting Kit-8

LSCC cell proliferation was examined using CCK-8 (Abcam, Cambridge, UK). Followed by LSCC cells were harvested, CCK-8 reagent (10 μl) was added to LSCC cells for 3 h at each time point. Absorbances (450 nm) were tested using microplate readers (ThermoFisher Scientific).

2.7. EdU analysis

LSCC cells (5×10^4) were seeded into 24-well plates and cultured for 24 h. Soon after, cells were grown in a serum-free DMEM medium with EdU (10 μmol/l, RiboBio) for 1.5 h. Followed by cells were fixed using 4% paraformaldehyde (Beyotime, Shanghai, China), and cells were stained with DAPI (Abcam) in line with manufacturer's protocol. Ultimately, all images were obtained under inverted fluorescence microscopy (ThermoFisher Scientific).

2.8. Western blot

After harvesting LSCC cells, total proteins were extracted with lysis buffer (Sigma-Aldrich, Missouri) with protease inhibitor (Abcam). Protein contents were tested with BCA Protein Assay Kits (Abcam). Total proteins were electroporated into PVDF membranes. Followed by membranes were blocked, membranes were exposed to primary antibodies against cleaved caspase 3 (ab32042, 1/500), Bax (ab32503, 1/1000), Bcl-2 (ab32124, 1/1000), Nanog (ab109250, 1/1000), OCT4 (ab200834, 1/10000), SOX2 (ab92494, 1/1000), LASP1 (ab156872, 1/10000), and β-actin (ab8226, 1 μg/ml). All antibodies were from Abcam. Membranes were further exposed to secondary antibodies. All protein bands were quantified by ECL Kits (Millipore).

2.9. Flow cytometry

LSCC cell apoptosis was examined using Annexin V-FITC/PI Apoptosis Detection Kits (Vazyme, Nanjing, China). LSCC cells were collected and fixed with 4% paraformaldehyde. Cells were further exposed to Annexin V-FITC (5 μl) and PI (5 μl) for 10 min. Apoptotic cells were determined using flow cytometry (ThermoFisher Scientific).

2.10. Sphere formation assay

LSCC cells were collected and coated as a single-cell suspension at a density of 200 cells per well on 96-well plates. After 10–12 days of culture, the number of spheres was counted under a microscope (ThermoFisher Scientific). Sphere formation efficiency was counted as a number of spheres formed divided by an initial number of single cells plated [18].

2.11. Transwell analysis

LSCC cell migration and invasion abilities were assessed using Transwell chambers with pores (8 μm, Corning, USA). For migration analysis, LSCC cells (5×10^4) were added to upper chambers, and DMEM containing 10% FBS was added to lower chambers. Twenty-four hours later, cells in lower chambers were fixed and dyed with 0.1% crystal violet (Beyotime). For invasion analysis, polycarbonate membranes pre-coated with Matrigel matrix (Nwbiotec, Beijing, China) were applied. Cells were observed and assessed under a microscope (ThermoFisher Scientific).

2.12. Dual-luciferase reporter analysis

CircSLC7A11 (wild-type and mutant) sequences, wild-type LASP1, mutant LASP1 were cloned into PmirGLO reporter vectors. After LSCC cells were cotransfected by miR-877-5p mimic and/or pcDNA-circSLC7A11, luciferase activities were conducted with commercial Kits (Promega, Wisconsin, USA). Relative activity of firefly luciferase in reporter vectors was normalized to Renilla luciferase control vector [19].

2.13. RNA pull-down

Followed by LSCC cell lysate was obtained using IP lysis buffer (Novobiotec), lysate was incubated with biotinylated-circSLC7A11 oligo. Then, mixture was exposed to streptavidin magnetic beads (ThermoFisher Scientific). Magnetic beads were pulled down and then washed. Input and pull-down eluents were edulcorated using Trizol (ThermoFisher Scientific) following manufacturer's standard procedure, and miR-877-5p levels were further measured.

2.14. RNA immunoprecipitation

LSCC cells were gathered and re-suspended in RIPA lysis buffer (Beyotime) with protease inhibitor. Then, cell lysates were incubated with anti-Ago2 (ab186733, 1:200), anti-IgG (ab186733, 1:500), and protein A/G magnetic beads (Novobiotec, Beijing, China) at 4 °C overnight. Followed by beads were washed, beads were incubated with protease K (Beyotime). CircSLC7A11 and miR-877-5p expressions were further tested.

2.15. Statistical analysis

Data are displayed as mean ± SD. Statistical comparisons among two groups, or exceeding two groups were evaluated with the Student's t-test, or ANOVA followed by Post Hoc Test (Least Significant Difference). Relevance of LSCC clinicopathological with circSLC7A11 was assessed using chi-square test. A *P*-value of <0.05 was considered statistically significant.

3. Results

3.1. CircSLC7A11 is overexpressed in LSCC

To investigate the relevance between circSLC7A11 and LSCC, circSLC7A11 expressions in LSCC tissues were tested. As displayed in Fig. 1A, remarkably high levels of circSLC7A11 were validated in LSCC clinical samples (n = 68). Furthermore, circSLC7A11 expressions were raised in LSCC (TNM stage III, n = 38) compared with TNM stages I + II (Fig. 1B, n = 30). Also, LSCC patients with high circSLC7A11 expressions owned short overall survival (Fig. 1C). By assessing the association between circSLC7A11 and clinical pathological features of LSCC, we corroborated that high circSLC7A11 expressions were interrelated to the TNM stage and T-category, but not interrelated to age, gender, tumor size, lymphatic metastasis of LSCC patients (Table 2). Moreover, circSLC7A11 expressions in LSCC cells were more than four times that in NP69 cells (Fig. 1D). Conclusively, circSLC7A11 was highly expressed in LSCC.

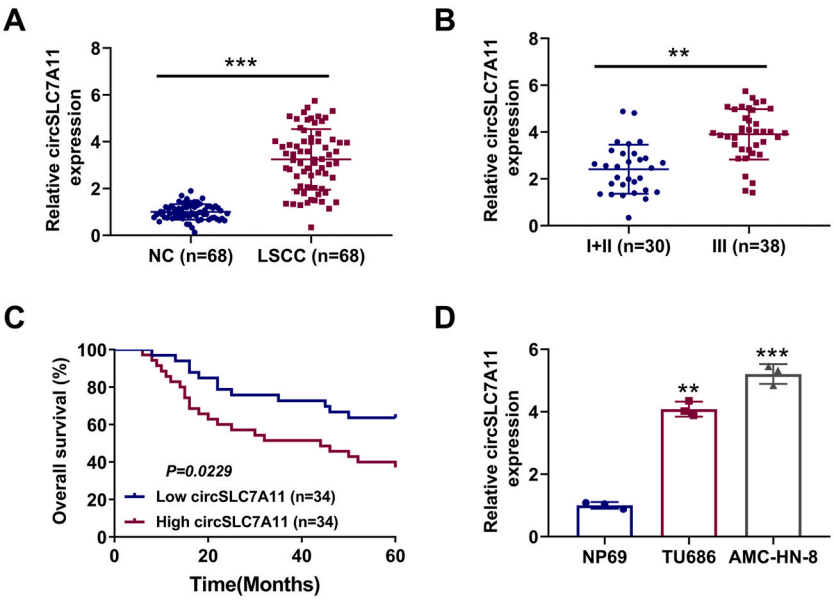

Fig. 1. Analysis of circSLC7A11 expression in LSCC. (A) CircSLC7A11 expressions in LSCC clinical samples (n = 68) and paracancerous tissues (n = 68) were tested using quantitative real-time PCR (qRT-PCR). (B) Comparison of circSLC7A11 expressions in LSCC (TNM stage III, n = 38) and TNM stages I + II (n = 30) using qRT-PCR. (C) Kaplan-Meier of relevance between circSLC7A11 expressions, and LSCC patients' survival time (n = 68). (D) Detection of circSLC7A11 expressions in LSCC cells and human nasopharyngeal epithelial cells (NP69). $^{**}P < 0.01$ vs. I + II (n = 30) and NP69. $^{***}P < 0.001$ vs. NC (n = 68) and NP69. NC: negative control.

3.2. CircSLC7A11 loss represses LSCC cell proliferation and enhanced cell apoptosis

To further estimate the circSLC7A11 function in LSCC, sh-circSLC7A11#1, sh-circSLC7A11#2, or sh-circSLC7A11#3 was transfected to LSCC cells and knockdown efficiency was verified (Fig. 2A). Among them, the sh-circSLC7A11#1 (named sh-circSLC7A11) knockdown efficiency was the highest in LSCC cells, and circSLC7A11 was lessened by nearly four-fifths in LSCC cells (Fig. 2A). On this basis, we further authenticated that silencing circSLC7A11 restrained LSCC cell proliferation (Fig. 2B). Also, EdU staining displayed a similar trend in LSCC cell proliferation (Fig. 2C). LSCC cell apoptosis was enhanced after circSLC7A11 knockdown (Fig. 2D). Western blot analysis expounded that circSLC7A11 loss raised cleaved caspase 3, Bax levels, lessened Bcl-2 levels (Fig. 2E). In short, interference with circSLC7A11 reduced LSCC cell proliferation and promoted cell apoptosis.

3.3. CircSLC7A11 knockdown reduces stemness characteristics, migration and invasion of LSCC cells

Sphere formation assay is a prominent method to identify the stemness of tumor cells [18]. As emerged in Fig. 3A, silencing circSLC7A11 reduced sphere formation efficiency. Subsequently, stemness-associated proteins Nanog, OCT4, and SOX2 expressions were lessened after silencing circSLC7A11 (Fig. 3B). Meanwhile, migration and invasion abilities of LSCC cells were attenuated after circSLC7A11 knockdown (Fig. 3C–D). To sum up, circSLC7A11 knockdown restrained stemness characteristics of LSCC cells.

3.4. CircSLC7A11 targets miR-877-5 p

Subsequently, we further evaluated the circSLC7A11 mechanism mediating LSCC progression. Starbase analysis predicted that circSLC7A11 contained the binding sites of miR-877-5p (Fig. 4A). Then, miR-877-5p was overexpressed in LSCC cells, and overexpression efficiency was verified (Fig. 4B). We further identified that miR-877-5p overexpression lessened the luciferase activity in circSLC7A11-WT, and owned no obvious influence on circSLC7A11-MUT (Fig. 4C). Also, RNA pull-down analysis expounded that the biotinylated circSLC7A11 probe enriched more miR-877-5p (Fig. 4D). RIP assay further demonstrated that circSLC7A11 and miR-877-5p were preferentially accumulated in miRNPs containing AGO2 (Fig. 4E). Meanwhile, miR-877-5p was lowly expressed in LSCC (Fig. 4F), and circSLC7A11 was negatively interrelated to miR-877-5p (Fig. 4G). Taken together, circSLC7A11 interacted with miR-877-5p.

3.5. MiR-877-5p regulates LASP1

MiR-877-5p target genes were further predicted and we discovered miR-877-5p binding sites in 3′untranslated regions of LASP1 (Fig. 5A). Meanwhile, transfecting miR-877-5p mimic lessened LASP1-WT luciferase activity, and owned no notable influence on LASP1-MUT (Fig. 5B). After circSLC7A11 was overexpressed in LSCC cells (Fig. 5C), we further confirmed that miR-877-5p mimic reduced the relative luciferase activity in LASP1-WT, while this reduction was abolished after circSLC7A11 overexpression (Fig. 5D). Furthermore, LASP1 expressions were elevated in LSCC tissues (Fig. 5E). Also, LASP1 was negatively correlated with miR-877-5p, and was positively correlated with circSLC7A11 in LSCC tissues (Fig. 5F–G). Moreover, transfecting miR-877-5p mimic lessened LASP1 protein levels by nearly three-quarters (Fig. 5H). Then, we confirmed that miR-877-5p inhibitor decreased its expressions, implying that miR-877-5p was successfully knocked down (Fig. 5I). On this basis, LASP1 protein levels were increased after miR-877-5p

Table 2
Relevance between circSLC7A11 and LSCC patients pathological features.

Characteristic	All cases	circSLC7A11 expression		P-value
		High (n = 34)	Low (n = 34)	
Age (years)				0.625
<60	38	18	20	
≥60	30	16	14	
Gender				0.329
Male	30	17	13	
Female	38	17	21	
Tumor size (cm)				0.618
<5	26	12	14	
≥5	42	22	20	
Lymphatic metastasis				0.088
Yes	37	22	15	
No	31	12	19	
TNM stages				0.002**
I + II	33	10	23	
III	35	24	11	
T-category				0.028*
T1-T2	31	11	20	
T3-T4	37	23	14	

A chi-square test was used for comparing groups between low and high circSLC7A11 expressions. *$P < 0.05$, **$P < 0.01$.

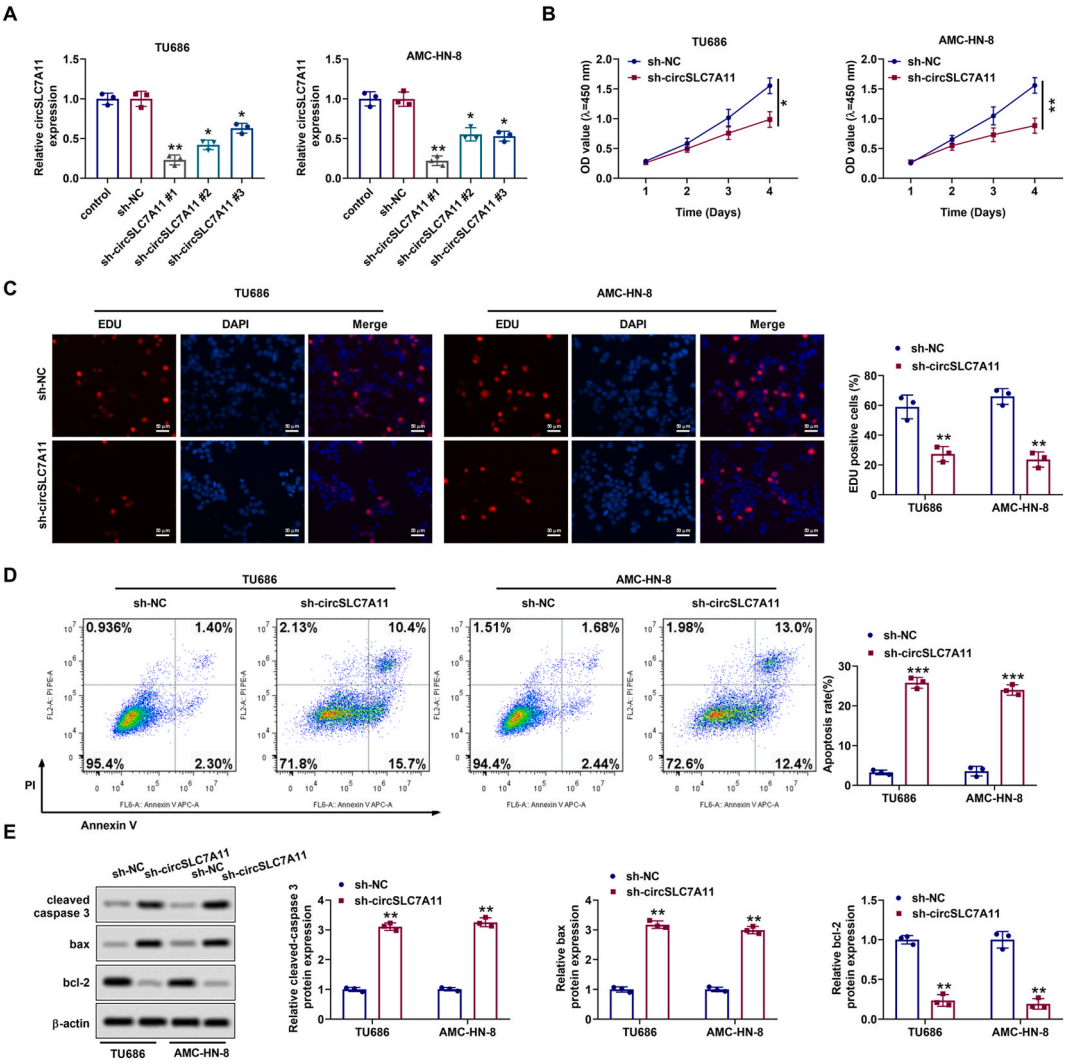

Fig. 2. Influence of circSLC7A11 knockdown on LSCC cell proliferation and apoptosis. (A) Sh-circSLC7A11#1, sh-circSLC7A11#2, or sh-circSLC7A11#3 were transfected to LSCC cells. CircSLC7A11 expressions were tested via qRT-PCR. (B) Sh-circSLC7A11#1 (sh-circSLC7A11) was transfected to LSCC cells for 48 h. Analysis of LSCC cell proliferation using Cell Counting Kit-8 (CCK-8). (C) LSCC cell proliferation was assessed via EdU analysis (scale bar: 50 μm). (D) LSCC cell apoptosis was examined using flow cytometry. (E) Apoptosis-related proteins (cleaved caspase 3, Bax, and Bcl-2) levels were tested via Western blot. $^{*}P < 0.05$, $^{**}P < 0.01$, $^{***}P < 0.001$ vs. control, sh-NC.

knockdown (Fig. 5J). We further clarified that circSLC7A11 knockdown reduced LASP1 protein levels, whereas miR-877-5p inhibitor co-transfection reversed this reduction (Fig. 5K). In summary, LASP1 functioned as an miR-877-5p target gene.

3.6. CircSLC7A11 regulates LSCC progression through miR-877-5p/LASP1

Next, we validated the circSLC7A11/miR-877-5p/LASP1 function in mediating LSCC. As exhibited in Fig. 6A, transfection of si-LASP1 (si-LASP1#1, si-LASP1#2, and si-LASP1#3) decreased LASP1 protein levels in LSCC cells, prompting that LASP1 was effectively knocked down in LSCC cells. Meanwhile, si-LASP1#1 owned the highest knockdown efficiency, so it was applied in following research (Fig. 6A). CCK-8 analysis corroborated that transfecting miR-877-5p inhibitor reversed the low LSCC cell proliferation induced by circSLC7A11 knockdown, and this trend was further reversed by LASP1 knockdown (Fig. 6B). Moreover, miR-877-5p knockdown lessened cleaved caspase 3, Bax, and raised Bcl-2, Nanog, OCT4, SOX2, while silencing LASP1 abolished these effects (Fig. 6C–D). All in all, circSLC7A11 enhanced LSCC malignant progression by mediating miR-877-5p/LASP1.

4. Discussion

LSCC is characterized by local recurrence that seriously restricts LSCC therapy [20,21]. Thus, expanding our understanding of LSCC

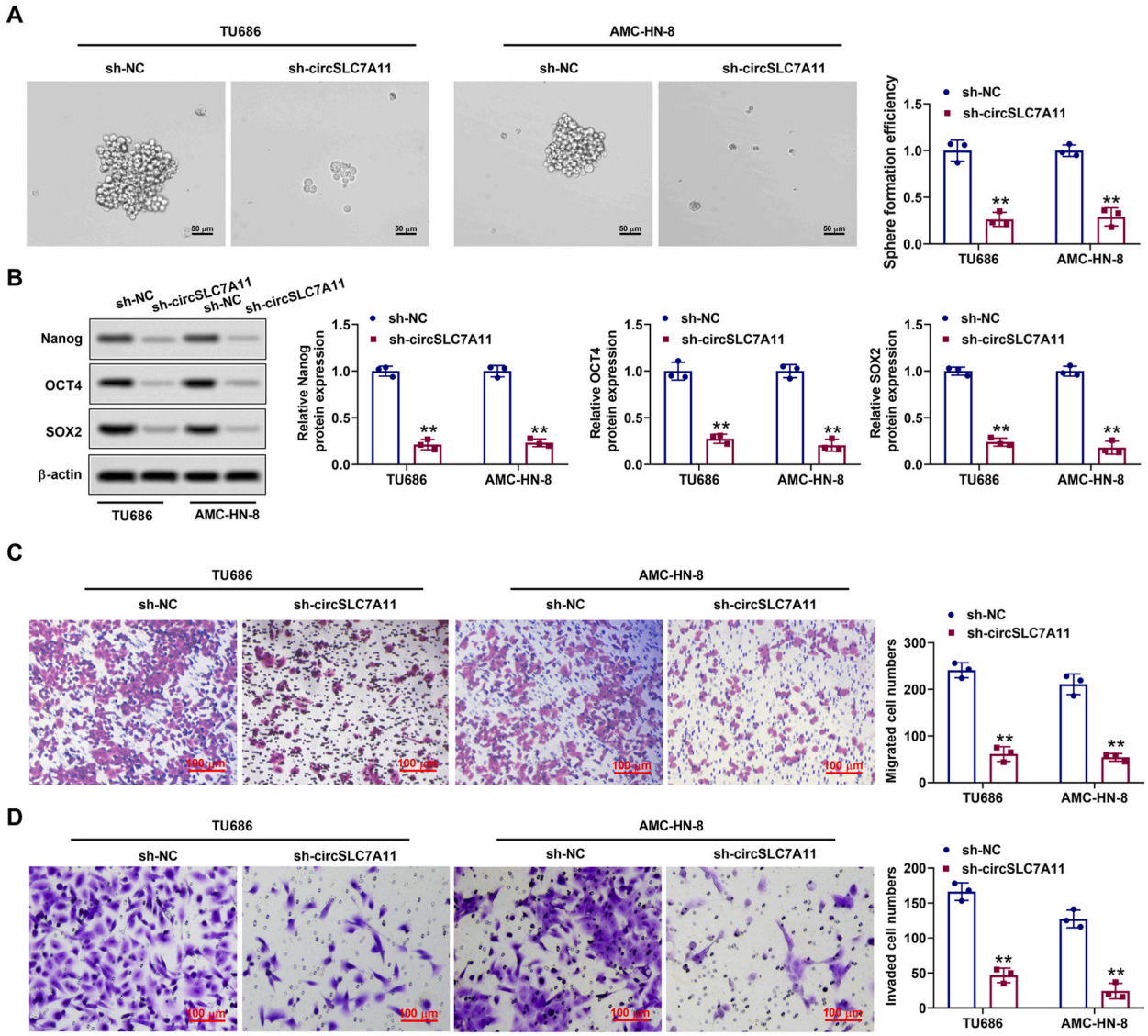

Fig. 3. CircSLC7A11 mediates stemness characteristics, migration and invasion of LSCC cells. sh-circSLC7A11 was transfected to LSCC cells for 48 h. (A) Sphere formation efficiency of LSCC cells was determined with sphere formation assay (scale bar: 50 μm). (B) Protein levels of stemness-associated proteins (Nanog, OCT4, and SOX2) were measured using Western blot. (C–D) Migration and invasion abilities of LSCC cells were assessed using Transwell analysis (scale bar: 100 μm). $^{**}P < 0.01$ vs. sh-NC.

mechanisms provides effective targets for LSCC clinical therapy. Given the accumulated evidence supporting the critical functions of circRNAs in tumors [22], we sought to investigate more circRNAs in LSCC. Here, we identified a novel circrNA circSLC7A11, and verified that circSLC7A11 expressions were raised in LSCC. As reported, circSLC7A11 is positively interrelated to tumor size and the TNM stage of hepatocellular carcinoma [14]. Similarly, our data illustrated that high circSLC7A11 expressions were bound up with the TNM stage. Functional studies further revealed that circSLC7A11 loss reduced LSCC cell proliferation, migration, invasion, stemness characteristics, and enhanced cell apoptosis. Also, mechanistic study results elucidated that circSLC7A11 contributed to LSCC by sponging miR-877-5p from LASP1. To the best of our knowledge, this study was the first to investigate the function and regulatory mechanism of circSLC7A11 in LSCC.

Previous studies clarify that circRNAs mediate various biological processes, especially in mediating tumor development [23,24]. A previous study reveals differentially expressed circRNAs in LSCC, implying that circRNAs exert momentous functions in LSCC [25]. Similarly, this study identified a novel circRNA and preliminarily confirmed that circSLC7A11 was dramatically overexpressed in LSCC. Also, we further revealed that high circSLC7A11 expressions were interrelated to the TNM stage of LSCC. Meanwhile, we corroborated that interference with circSLC7A11 attenuated LSCC cell proliferation, migration, invasion, and enhanced cell apoptosis through function loss studies. Accumulating research illustrates that stemness is an important pathological feature of LSCC

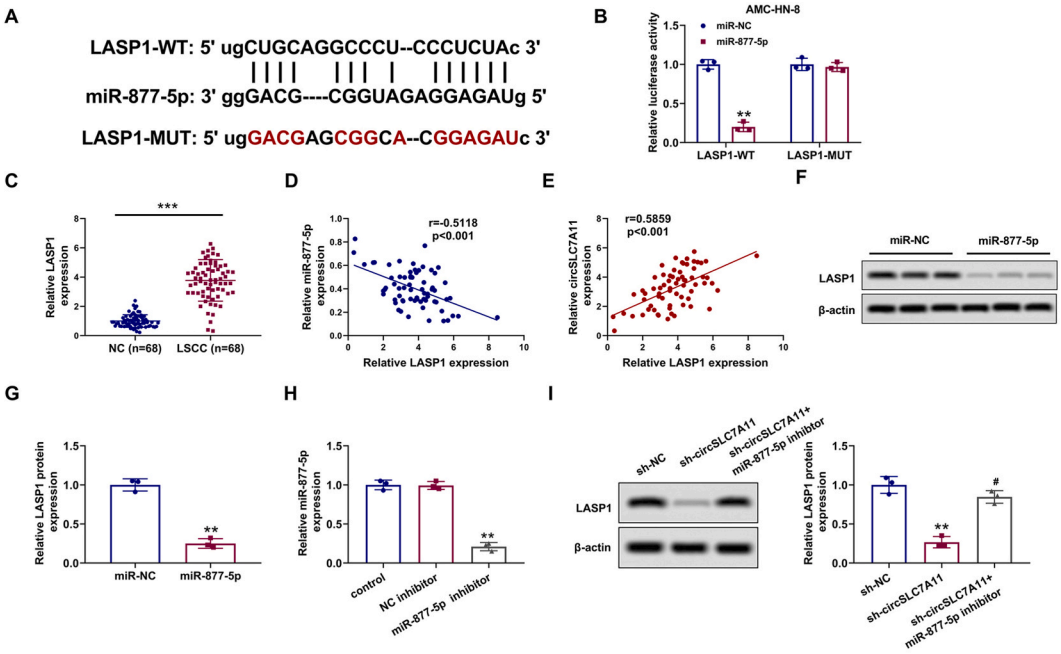

Fig. 4. Validation of circSLC7A11 targeting miR-877-5p. (A) Starbase predicted that circSLC7A11 had miR-877-5p connection sites. (B) MiR-877-5p mimic was transfected to LSCC cells for 48 h. MiR-877-5p expressions were measured via qRT-PCR. (C) Analysis of luciferase activity in LSCC cells using dual-luciferase reporter. (D) Connection between circSLC7A11 and miR-877-5p was assessed by RNA pull-down. (E) Interaction between circSLC7A11 and miR-877-5p was illustrated using RNA Immunoprecipitation. (F) Comparison of miR-877-5p expressions in LSCC clinical samples (n = 68) and paracancerous tissues (n = 68). (G) Correlation of circSLC7A11 and miR-877-5p was illustrated. $^{**}P < 0.01$ vs. miR-NC. $^{***}P < 0.001$ vs. miR-NC, oligo probe, anti-IgG, and NC.

development [26,27]. Sphere formation assay is a prominent method to identify the stemness of tumor cells [28]. Our experimental data revealed that silencing circSLC7A11 reduced sphere formation efficiency, suggesting that circSLC7A11 knockdown restrained LSCC cell stemness characteristics. Nanog, OCT4, and SOX2 are stemness characteristics-related makers that are commonly applied to indicate tumor development [29,30]. As expected, our study expounded that circSLC7A11 knockdown reduced Nanog, OCT4, and SOX2 expressions in LSCC cells, prompting that circSLC7A11 knockdown repressed stemness characteristics of LSCC cells. The above findings suggested that circSLC7A11 exerted a cancer-promoting function in LSCC.

Subsequently, we sought to elucidate the molecular mechanism of circSLC7A11 in LSCC. Emerging evidence illustrates that circRNAs reduce the inhibitory influences of microRNA (miRNA) on target genes by absorbing miRNAs [31,32]. MiRNAs are another group of non-coding RNAs that participate in LSCC biological process. For instance, ectopic miR-29a reduces LSCC growth, and miR-29a regards as a tumor suppressor in LSCC via STAT3 [33]; miR-139-3p mimic restrains LSCC cell proliferation, and RAB5a overexpression reverses the influence of miR-139-3p on LSCC [34]. Critically, emerging evidence suggests that competing endogenous RNA (ceRNA) pattern mediates LSCC progression. For instance, hsa_circ_0042823 knockdown reduces LSCC tumor growth through miR-877-5p/FOXM1 [35]. Hsa_circ_0023305 aggravates LSCC by regulating TRPM7 through sponging miR-218-5p [36]. Critically, miR-877-5p is mediated by hsa_circ_0061395 in hepatocellular carcinoma [37], and circPRH1-PRR4 in NSCLC [38]. Here, we authenticated circSLC7A11 targeted miR-877-5p. Meanwhile, our experiments further confirmed that circSLC7A11 and miR-877-5p expressions were dramatically negatively correlated in LSCC tissues, implying that circSLC7A11 might exert ceRNA functions in LSCC by absorbing miR-877-5p.

Considering relevance between circSLC7A11 and miR-877-5p, we further explored probable miR-877-5p targets. Our studies identified LASP1 as a downstream regulatory target of miR-877-5p. LASP1 is first identified in lymph nodes of breast cancer patients [39]. LASP1 gene is located on chromosome 17q11–21.3 and encodes a protein with 261 amino acids [40]. With a continuous exploration of physiological and pathological functions of LASP1, it has been widely recognized that LASP1 has potential to become a cancer biomarker [41,42]. Moreover, another study confirms that high LASP1 expressions accelerate LSCC development, hinting that LASP1 is a potential target in the progression of LSCC [43]. Additionally, LASP1 is regulated by multiple miRNAs containing miR-133 [44], miR-377-3p [45], and miR-143 [46]. Similarly, we revealed that LASP1 was overexpressed in LSCC, and LASP1 expressions were positively interrelated to circSLC7A11 and negatively interrelated to miR-877-5p. Furthermore, our rescue assays demonstrated that circSLC7A11 regulated LSCC progress through miR-877-5p/LASP1.

5. Conclusion

CircSLC7A11 bound to miR-877-5p to mediate LASP1 in LSCC. Meanwhile, we confirmed that targeting circSLC7A11 might be a

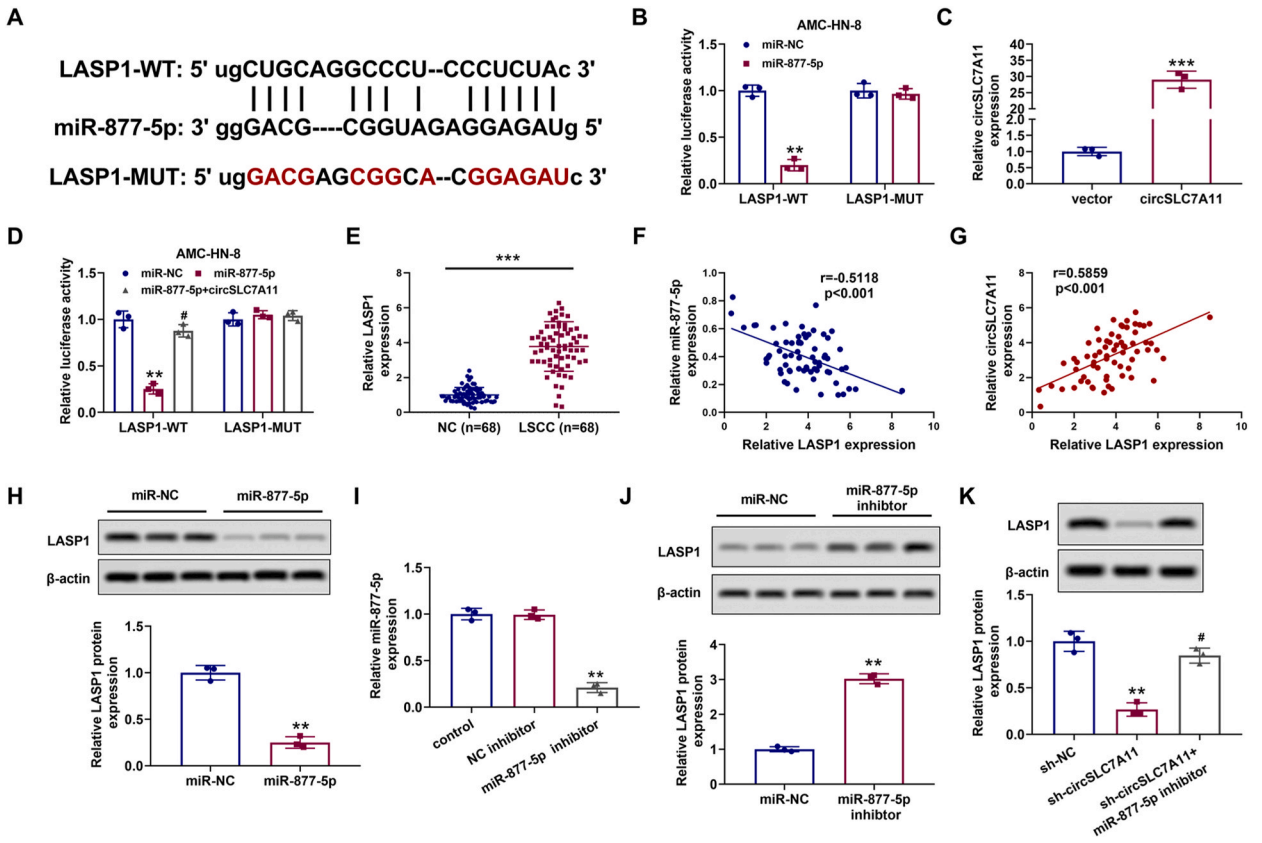

Fig. 5. MiR-877-5p interacts with LASP1. (A) MiR-877-5p connection sites in 3′untranslated regions of LASP1 were forecasted via Starbase. (B) Luciferase activity was assessed using dual-luciferase reporter analysis. (C) PcDNA-circSLC7A11 was transfected to LSCC cells for 48 h. Detection of circSLC7A11 expressions using qRT-PCR. (D) MiR-877-5p mimic and/or pcDNA-circSLC7A11 was transfected to LSCC cells for 48 h. The luciferase activity in LSCC cells was examined with a dual-luciferase reporter. (E) Detection of the LASP1 expressions in LSCC clinical samples (n = 68) and paracancerous tissues (n = 68). (F–G) Correlation of LASP1 and miR-877-5p, LASP1 and circSLC7A11 was evaluated using qRT-PCR. (H) MiR-877-5p mimic was transfected to LSCC cells for 48 h. Analysis of the LASP1 protein levels by Western blot. (I) MiR-877-5p inhibitor was transfected to LSCC cells for 48 h. MiR-877-5p expressions were tested using qRT-PCR. (J) LASP1 protein levels were measured using Western blot. (K) Sh-circSLC7A11 and/or miR-877-5p inhibitor was transfected to LSCC cells for 48 h. Detection of the LASP1 protein levels. $^{**}P < 0.01$ vs. miR-NC, NC inhibitor, and sh-NC. $^{***}P < 0.001$ vs. vector, NC. $^{\#}P < 0.05$ vs. sh-circSLC7A11.

novel insight for a therapeutic strategy for LSCC. Also, the deficiencies of this research were presented: (1) this study only conducted a loss-of-function assay; (2) this study did not conduct in-depth clinical research, and a one-way/multivariate analysis of variance was needed to determine whether circSLC7A11 was an independent prognostic factor for LSCC; (3) the circSLC7A11/miR-877-5p/LASP1 function in tumorigenesis in animal models was not investigated; (4) this study did not investigate the effect of circSLC7A11 on angiogenesis and tumor metastasis in LSCC *in vivo*. We would conduct in-depth research to enrich the content.

Declarations

Author contribution statement

WenJie Yu: Performed the experiments; Analyzed and interpreted the data.
XiaoLing He: Analyzed and interpreted the data.
ChunMing Zhang: Contributed reagents, materials, analysis tools or data.
FuHui Huang: Conceived and designed the experiments; Wrote the paper.

Data availability statement

Data will be made available on request.

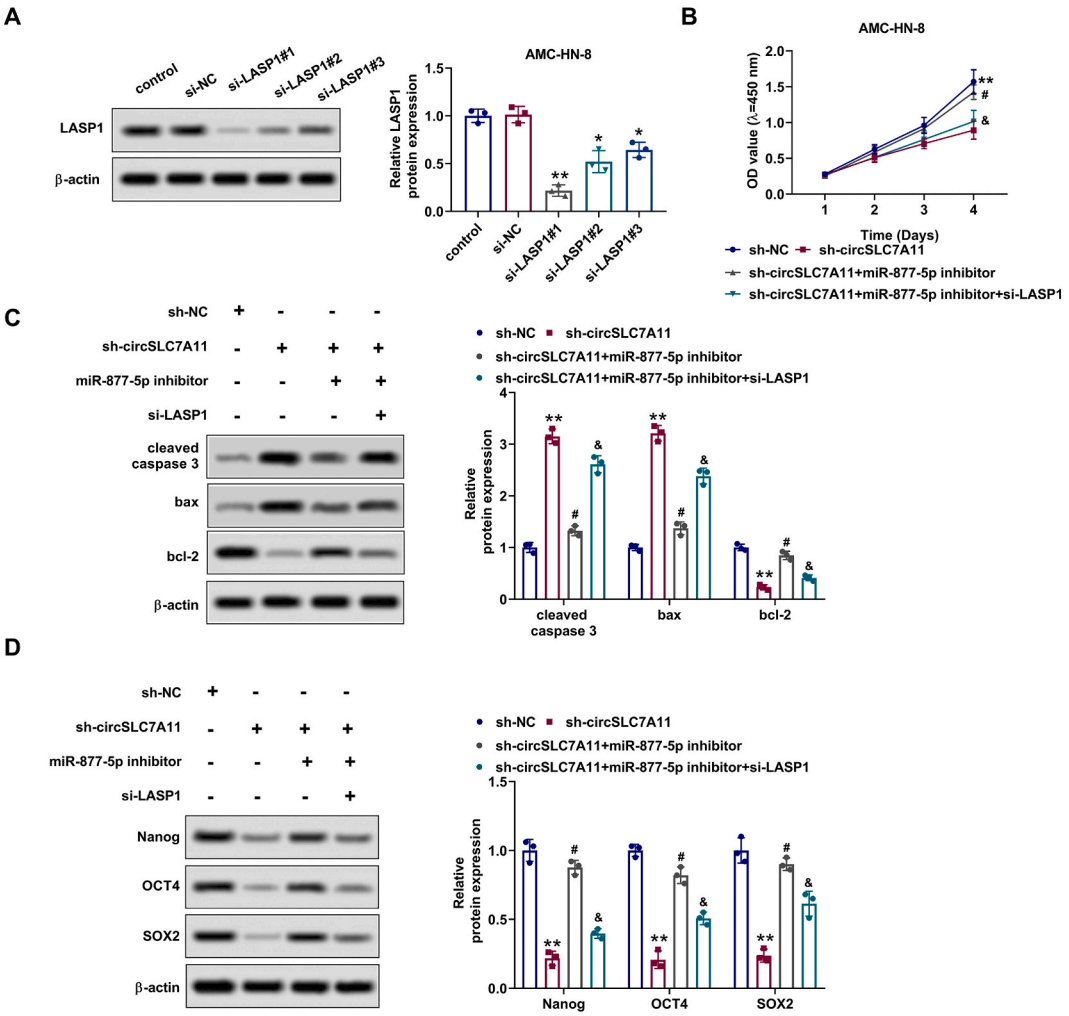

Fig. 6. CircSLC7A11 influences LSCC progression by miR-877-5p/LASP1. (A) Si-LASP1#1, #2, or #3 transfected to LSCC cells for 48 h. LASP1 levels were tested. (B) After sh-circSLC7A11 was transfected to LSCC cells for 48 h, miR-877-5p inhibitor and/or si-LASP1 were transfected to LSCC cells for 48 h. Analysis of LSCC cell proliferation using CCK-8 assay. (C–D) Protein levels of cleaved caspase 3, Bax, Bcl-2, Nanog, OCT4, and SOX2 were tested. $^{*}P < 0.05$ vs. control. $^{**}P < 0.01$ vs. control, sh-NC. $^{\#}P < 0.05$ vs. sh-circSLC7A11. $^{\&}P < 0.05$ vs. sh-circSLC7A11+miR-877-5p inhibitor.

Declaration of competing interest

The authors declare that they have no known competing financial interests or personal relationships that could have appeared to influence the work reported in this paper.

Appendix A. Supplementary data

Supplementary data to this article can be found online at https://doi.org/10.1016/j.heliyon.2023.e18290.

References

[1] M. Sun, S. Chen, M. Fu, Model establishment of prognostic-related immune genes in laryngeal squamous cell carcinoma, Medicine (Baltim.) 100 (2) (2021), e24263.
[2] K. Metzger, et al., A six-gene expression signature related to angiolymphatic invasion is associated with poor survival in laryngeal squamous cell carcinoma, Eur. Arch. Oto-Rhino-Laryngol. 278 (4) (2021) 1199–1207.
[3] C.E. Steuer, et al., An update on larynx cancer, CA A Cancer J. Clin. 67 (1) (2017) 31–50.
[4] E. Tsiambas, et al., c-Jun/c-Fos complex in laryngeal squamous cell carcinoma, J. Buon. 25 (2) (2020) 618–620.

[5] V. Vander Poorten, et al., Salvage surgery for residual or recurrent laryngeal squamous cell carcinoma after (Chemo)radiotherapy: oncological outcomes and prognostic factors, Eur. J. Surg. Oncol. 47 (11) (2021) 2711–2721.
[6] L. Xia, et al., Circular RNAs as biomarkers for cancer, Adv. Exp. Med. Biol. 1087 (2018) 171–187.
[7] S. Ghafouri-Fard, et al., CircMTO1: a circular RNA with roles in the carcinogenesis, Biomed. Pharmacother. 142 (2021), 112025.
[8] L.S. Kristensen, et al., Circular RNAs in cancer: opportunities and challenges in the field, Oncogene 37 (5) (2018) 555–565.
[9] I.L. Patop, S. Wüst, S. Kadener, Past, present, and future of circRNAs, EMBO J. 38 (16) (2019), e100836.
[10] X. Guo, et al., CircRNAs: promising factors for regulating angiogenesis in colorectal cancer, Clin. Transl. Oncol. 24 (9) (2022) 1673–1681.
[11] L.S. Kristensen, et al., The biogenesis, biology and characterization of circular RNAs, Nat. Rev. Genet. 20 (11) (2019) 675–691.
[12] D. Fan, Y. Zhu, Circ_0120175 promotes laryngeal squamous cell carcinoma development through up-regulating SLC7A11 by sponging miR-330-3p, J. Mol. Histol. 53 (2) (2022) 159–171.
[13] F. Chen, et al., Knockdown of circ_0001883 may inhibit epithelial-mesenchymal transition in laryngeal squamous cell carcinoma via the miR-125-5p/PI3K/AKT axis, Exp. Ther. Med. 22 (3) (2021) 1007.
[14] Y. Huang, et al., The circular RNA circSLC7A11 functions as a mir-330-3p sponge to accelerate hepatocellular carcinoma progression by regulating cyclin-dependent kinase 1 expression, Cancer Cell Int. 21 (1) (2021) 636.
[15] H.W. Chen, et al., The circular RNA circSlc7a11 promotes bone cancer pain pathogenesis in rats by modulating LLC-WRC 256 cell proliferation and apoptosis, Mol. Cell. Biochem. 476 (4) (2021) 1751–1763.
[16] L. Miao, et al., A novel circRNA-miRNA-mRNA network identifies circ-YOD1 as a biomarker for coronary artery disease, Sci. Rep. 9 (1) (2019), 18314.
[17] L. Kalaimani, et al., Hsa-miR-143-3p inhibits Wnt-β-catenin and MAPK signaling in human corneal epithelial stem cells, Sci. Rep. 12 (1) (2022), 11432.
[18] L. Wang, et al., Zoledronic acid inhibits the growth of cancer stem cell derived from cervical cancer cell by attenuating their stemness phenotype and inducing apoptosis and cell cycle arrest through the Erk1/2 and Akt pathways, J. Exp. Clin. Cancer Res. 38 (1) (2019) 93.
[19] D. Hudy, J. Rzeszowska-Wolny, Expression of miRNA-targeted and not-targeted reporter genes shows mutual influence and intercellular specificity, Int. J. Mol. Sci. 23 (23) (2022).
[20] P. Pakkanen, et al., T1 glottic laryngeal cancer: the role of routine follow-up visits in detecting local recurrence, Eur. Arch. Oto-Rhino-Laryngol. 278 (12) (2021) 4863–4869.
[21] R.S. Voora, et al., Patterns of failure after definitive treatment of T4a larynx cancer, Otolaryngol. Head Neck Surg. 167 (2) (2022) 274–285.
[22] L.S. Kristensen, et al., The emerging roles of circRNAs in cancer and oncology, Nat. Rev. Clin. Oncol. 19 (3) (2022) 188–206.
[23] Y. Yin, et al., Emerging roles of circRNA in formation and progression of cancer, J. Cancer 10 (21) (2019) 5015–5021.
[24] K.Y. Hsiao, et al., Noncoding effects of circular RNA CCDC66 promote colon cancer growth and metastasis, Cancer Res. 77 (9) (2017) 2339–2350.
[25] C. Lu, et al., RNA-Seq profiling of circular RNAs in human laryngeal squamous cell carcinomas, Mol. Cancer 17 (1) (2018) 86.
[26] R. Li, et al., Long noncoding RNA FOXD2-AS1 enhances chemotherapeutic resistance of laryngeal squamous cell carcinoma via STAT3 activation, Cell Death Dis. 11 (1) (2020) 41.
[27] J. Wang, et al., LY6D as a chemoresistance marker gene and therapeutic target for laryngeal squamous cell carcinoma, Stem Cell. Dev. 29 (12) (2020) 774–785.
[28] Q. Tang, et al., TM4SF1 promotes EMT and cancer stemness via the Wnt/β-catenin/SOX2 pathway in colorectal cancer, J. Exp. Clin. Cancer Res. 39 (1) (2020) 232.
[29] D. Pedregal-Mallo, et al., Prognostic significance of the pluripotency factors NANOG, SOX2, and OCT4 in head and neck squamous cell carcinomas, Cancers 12 (7) (2020).
[30] M.C. Kuo, et al., Cancer stemness in bone marrow micrometastases of human breast cancer, Surgery 163 (2) (2018) 330–335.
[31] J. Zhang, et al., GreenCircRNA: a Database for Plant circRNAs that Act as miRNA Decoys, Database, Oxford), 2020, p. 2020.
[32] I.B. Filippenkov, et al., Circular RNAs-one of the enigmas of the brain, Neurogenetics 18 (1) (2017) 1–6.
[33] Y.B. Liu, et al., MicroRNA-29a functions as a tumor suppressor through targeting STAT3 in laryngeal squamous cell carcinoma, Exp. Mol. Pathol. 116 (2020), 104521.
[34] Y. Ma, et al., Anti-cancer effect of miR-139-3p on laryngeal squamous cell carcinoma by targeting rab5a: in vitro and in vivo studies, Pathol. Res. Pract. 216 (11) (2020), 153194.
[35] T. Wu, et al., Hsa_circ_0042823 accelerates cancer progression via miR-877-5p/FOXM1 axis in laryngeal squamous cell carcinoma, Ann. Med. 53 (1) (2021) 960–970.
[36] Y. Zhang, et al., hsa_circ_0023305 enhances laryngeal squamous cell carcinoma progression and modulates TRPM7 via miR-218-5p sponging, BioMed Res. Int. 2021 (2021), 9968499.
[37] Y. Yu, et al., Circular RNA hsa_circ_0061395 accelerates hepatocellular carcinoma progression via regulation of the miR-877-5p/PIK3R3 axis, Cancer Cell Int. 21 (1) (2021) 10.
[38] J. Ma, Q. Li, Y. Li, CircRNA PRH1-PRR4 stimulates RAB3D to regulate the malignant progression of NSCLC by sponging miR-877-5p, Thor. Canc. 13 (5) (2022) 690–701.
[39] C. Tomasetto, et al., Lasp-1 (MLN 50) defines a new LIM protein subfamily characterized by the association of LIM and SH3 domains, FEBS Lett. 373 (3) (1995) 245–249.
[40] E. Butt, C.M. Howard, D. Raman, LASP1 in cellular signaling and gene expression: more than just a cytoskeletal regulator, Cells 11 (23) (2022).
[41] V. Ruggieri, et al., Paving the path for invasion: the polyedric role of LASP1 in cancer, Tum. Biol. 39 (6) (2017), 1010428317705757.
[42] Q. Xue, et al., LASP1 induces epithelial-mesenchymal transition in lung cancer through the TGF-β1/smad/snail pathway, Cancer Res. J. 2021 (2021), 5277409.
[43] Y. Zheng, et al., Circ_0023028 contributes to the progression of laryngeal squamous cell carcinoma by upregulating LASP1 through miR-486-3p, Mol. Cell. Biochem. 476 (8) (2021) 2951–2961.
[44] Z. Huang, et al., miR-133 inhibits proliferation and promotes apoptosis by targeting LASP1 in lupus nephritis, Exp. Mol. Pathol. 114 (2020), 104384.
[45] Y. Liu, et al., LASP1 promotes glioma cell proliferation and migration and is negatively regulated by miR-377-3p, Biomed. Pharmacother. 108 (2018) 845–851.
[46] H. Liu, et al., miR-143 inhibits migration and invasion through regulating LASP1 in human esophageal cancer, Int. J. Clin. Exp. Pathol. 12 (2) (2019) 466–476.